Proceedings of the ASME 2009 Dynamic Systems and Control Conference
DSCC2009
October 12-14, 2009, Hollywood, California, USA

DSCC2009-2692

MODEL-BASED FAULT DETECTION AND DIAGNOSIS FOR ELECTROMAGNETIC VALVE DRIVES

Mark Beck
TU Darmstadt
Institute of Automatic Control
Darmstadt, Germany 64283
mbeck@iat.tu-darmstadt.de

Marco Muenchhof
TU Darmstadt
Institute of Automatic Control
Darmstadt, Germany 64283
mmuenchhof@iat.tu-darmstadt.de

Rolf Isermann
TU Darmstadt
Institute of Automatic Control
Darmstadt, Germany 64283
risermann@iat.tu-darmstadt.de

ABSTRACT

This paper describes the model-based fault detection and diagnosis for electromagnetic actuators. Due to hysteresis behavior, the model of Jiles and Atherton is used to capture these hysteretic effects. It is shown that the use of this model results in superior model fidelity and allows to detect even tiny, incipient faults at the actuator. The method has been applied to a direct-driven proportional valve of an electro-hydraulic servo axis and has been tested extensively on a real testbed.

INTRODUCTION

Electromagnetic actuators increasingly replace the traditional, purely mechanically, pneumatically, or hydraulically driven actuators. In the area of electro-hydraulic servo axes, directly driven proportional valves replace in many applications the two-stage valves with the traditional nozzle-flapper construction controlled by torque-motors. Wear and tear due to abrasion, erosion, and excessive temperature can severely degrade the operating time. Furthermore, the ongoing integration of electromagnetic actuators in mechatronic systems, puts even more emphasis on the need to detect and diagnose faults autonomously. Signal-based methods such as limit checking or trend checking, which so far have mostly been applied in industry, do not allow the detection of tiny, incipient faults. Typically, the fault becomes large without being detected and therefore, the plant must immediately be shut down when the fault is detected by classical methods. Using modern, process-model based methods, it is however possible to detect and diagnose faults in a much earlier stage and thus prevent the shutdown of the plant by means of fault-management methods, such as reconfiguration of the control, switching-over from a defect to an intact component. The paper will present the design of such a model-based fault detection and diagnosis system for electromagnetic drives.

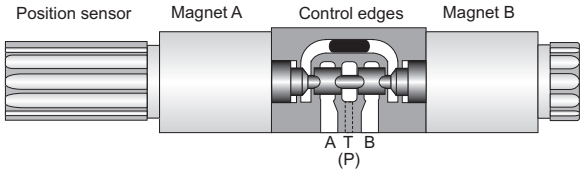

Figure 1. 4/3 PROPORTIONAL VALVE

Model-Based Fault Detection

Electromagnetic actuators contain different energy conversion mechanisms, [1]. First, the electric energy supplied to the actuator is converted into magnetic energy, which is subsequently converted into mechanical energy. Faults can affect the electro-magnetic conversion as well as the magneto-mechanic conversion. Therefore, in this paper a model is presented that covers both the electro-magnetic as well as the magneto-mechanic energy conversion. The model-based fault detection and diagnosis is developed for a direct driven proportional valve with four ports (see Figure 1) but it can be applied to many other electromagnetic actuators as well. The position of the valve slider affects the volume flow rate over the four control edges of the proportional valve. The position of the valve slider is measured with a linear variable differential transformer and is controlled by an underlying slider position controller. The two electromagnets allow to displace the slider continuously in both directions. The electro-magnetic part can be described by

$$u_{\mathrm{A}}(t) = R_{\mathrm{A}} i_{\mathrm{A}}(t) + \frac{\partial \psi_{\mathrm{A}}(x, i_{\mathrm{A}})}{\partial x}\frac{\partial x}{\partial t} + \frac{\partial \psi_{\mathrm{A}}(x, i_{\mathrm{A}})}{\partial i_{\mathrm{A}}}\frac{\partial i_{\mathrm{A}}}{\partial t} \qquad (1)$$

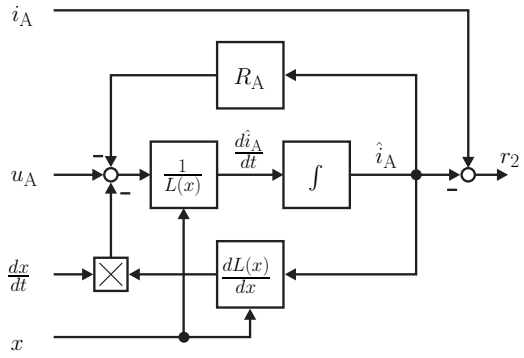

Figure 2. MODEL STRUCTURE RESIDUAL 2

$$u_B(t) = R_B i_B(t) + \frac{\partial \psi_B(x, i_B)}{\partial x}\frac{\partial x}{\partial t} + \frac{\partial \psi_B(x, i_B)}{\partial i_B}\frac{\partial i_B}{\partial t} \qquad (2)$$

with

R_A,R_B	:	resistance (magnet A, magnetB)
ψ_A, ψ_B	:	flux linkage (magnet A, magnet B)
u_A,u_B	:	coil voltage (magnet A, magnet B)
i_A,i_B	:	coil current (magnet A, magnet B).

The eletromagnets used in the direct-driven proportional valve at the testbed are common DC magnets without the adaption of the force-air gap characteristics (the matching spart of the armature is not optimized). Therefore the flux linkages can be simplified as

$$\psi_A(x, i_A) = i_A \cdot L_A(x) \qquad (3)$$
$$\psi_B(x, i_B) = i_B \cdot L_B(x). \qquad (4)$$

Equations 1 and 2 can be formulated as

$$u_A(t) = \left(R_A i_A(t) + i_A \cdot \frac{dL_A(x)}{dx}\frac{dx}{dt} + L_A(x)\frac{di_A}{dt} \right) \qquad (5)$$
$$u_B(t) = \left(R_B i_B(t) + i_B \cdot \frac{dL_B(x)}{dx}\frac{dx}{dt} + L_B(x)\frac{di_B}{dt} \right). \qquad (6)$$

In order to detect faults in the electro-magnetic part, two isolating residuals (also described in [8], [9]) can be formulated

$$r_2(t) = i_A - \hat{i}_A \qquad (7)$$
$$r_3(t) = i_B - \hat{i}_B. \qquad (8)$$

The residual r_2 describes the difference between the measured current i_A and the expected current $\hat{i}_A$ in coil A. The difference between the measured current i_B and the expected current $\hat{i}_B$ in coil B is described by the residual r_3 Figures 2 and 4 illustrate schematically the model structure of the residual 2 and 3. By identification techniques (least-square parameter estimation, prediction error minimization) and measurements on the testbed the model parameters are identified. In the fault-free case the residuals r_2 and r_3 are close to zero. Only noise and model uncertainty lead to small amplitudes. If a fault occurs inside the coil (e.g. partial winding short) or in the power electronics (e.g. faulty current sensor signal) the residuals deflect and a fault can be detected. For the control of electromagnets, one differentiates between voltage-based and current-based control. The advantages and disadvantages of the two control strategies are described in [1]. The dynamic model presented can be used for both control strategies. At the testbed the power supplies of the two electromagnets are realized as H-bridges. Thus, the voltages supplied to the two electromagnets resemble square waves and cause a permanent rise and fall of the currents. The current hence does not only contain a quasi-stationary DC part, but also a ripple. This ripple occurs under current-control as well as standard puls-width modulation control. The hysteretic effects on r_2 and r_3 can be neglected as the model fidelity is sufficient enough to detect critical faults in the electro-magnetic part of the valve. The

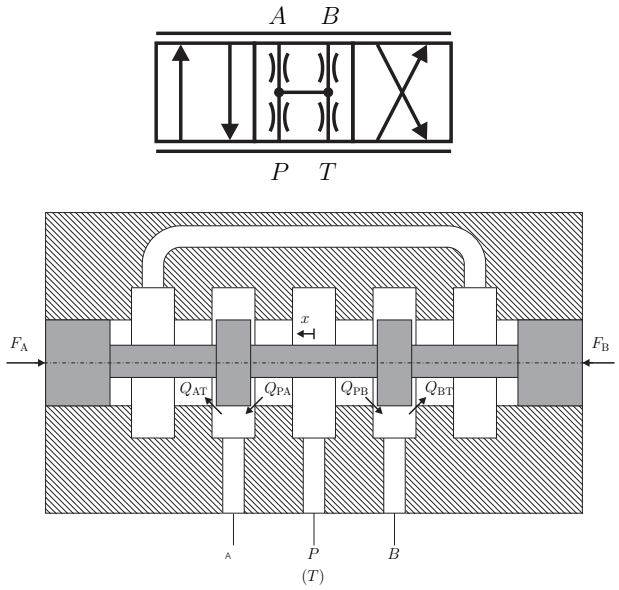

Figure 3. HYDRAULIC SCHEME OF 4/3 PROPORTIONAL VALVE

slider of the direct driven proportional valve controls the volume flows (Figure 3: Q_{PA},Q_{AT},Q_{PB} and Q_{BT}) over the conrol edges. Figure 3 shows the schematic assembly of the 4/3 slider valve. In order to detect faults in the magneto-mechanical part of the valve Newton's Second Law is considered. The equation

$$m\ddot{x} = F_B(x, i_B) - F_A(x, i_A) - d\dot{x} - cx - F_F - F_V \qquad (9)$$

with

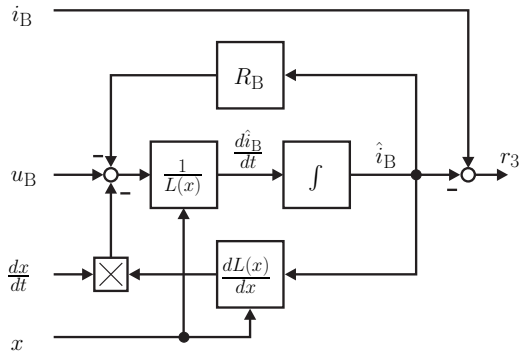

Figure 4. MODEL STRUCTURE RESIDUAL 3

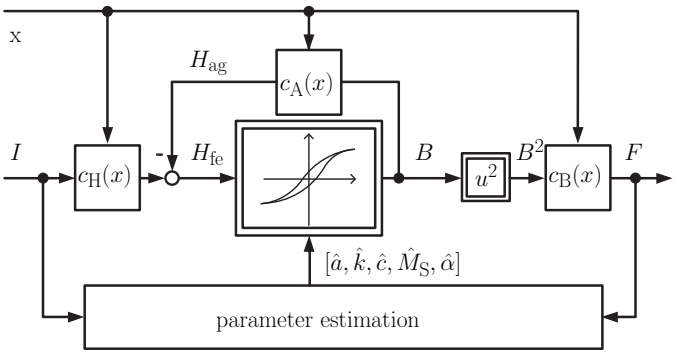

Figure 5. MODEL STRUCTURE

m	:	slider mass
d	:	damping constant
c	:	spring constant
F_F	:	friction force
F_V	:	flow forces

describes the forces exposed to the slider. Because the DC electromagnets can only induce either a compressive or a traction force, two electromagnets are required for positioning. In order to change the slider position the control law

$$I_A = I_0 - \Delta I \tag{10}$$

$$I_B = I_0 + \Delta I. \tag{11}$$

is used. This control law is well-known and is used in many other applications (e.g. magnetic bearings). Researches on the testbed show the need of a precise mathematical description of the non-linear hysteretic characteristics of the two DC electromagnets in order to detect small faults. Without modelling the hysteretic characteristics, only large faults in the magneto-mechanical part of the valve can be detected. Hysteresis effects [4] do not only influence the dynamics of electromagnets, but can also be found in many other actuators, such as e.g. piezo actuators. In many cases these hysteretic effects are neglected or simply modelled by using look-up tables. This however results in a low model fidelity. The Preisach model or the Jiles-Atherton model on the other hand provide a much higher model fidelity. Because of physical interpretability and a good proportion of computational effort and model fidelity the the Jiles-Atherton approach is chosen.

The Jiles-Atherton model is detailed explained in [5] and can be completely described by

$$H_E = H + \alpha M \tag{12}$$

$$M_{an} = M_S \left[\coth\left(\frac{H_E}{a}\right) - \frac{a}{H_E} \right] \tag{13}$$

$$\frac{dM}{dH} = c\frac{dM_{an}}{dH} + (1-c)\frac{M_{an} - M_{irr}}{\delta k - \alpha(M_{an} - M_{irr})} \tag{14}$$

$$\delta = \operatorname{sign}\frac{dH}{dt} \tag{15}$$

$$M = \int \frac{dM}{dH} dH \tag{16}$$

$$M = cM_{an} + (1-c)M_{irr} \tag{17}$$

$$B = \mu_0 (H + M) \tag{18}$$

with the parameters

α	:	interaction of domains
a	:	material-specific constant
k	:	pinning constant
M_S	:	saturation magnetisation
c	:	reversibility coefficient.

In order to map the *B-H* hysteresis onto a *F-I* hysteresis and thus model the current-force relation of the electromagnet, Maxwell's equation can be applied:

$$H_{fe} l_{fe} + H_{ag} l_{ag} = NI \tag{19}$$

H_{fe}	:	field strength (ferromagnetic circuit)
H_{ag}	:	field strength (air gap)
l_{fe}	:	ferromagnetic circuit length
l_{ag}	:	air gap length
N	:	number of turns.

The traction force of the magnet can be described by

$$F = \frac{B^2}{2\mu_0} A \tag{20}$$

μ_0	:	air permeability
A	:	active surface.

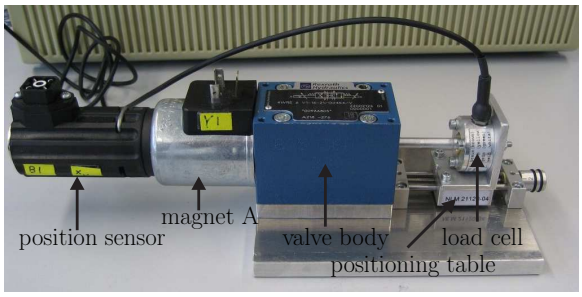

Figure 6. MEASUREMENT SETUP

Figure 5 shows the whole model structure. The inputs of the model are the current and the slider position. The output is the traction force of the DC electromagnet. With the help of the embedded Jiles-Atherton model the hysteretic magnetic field intensity versus the flux density characteristic is considered. The parameters $c_{\mathrm{H}}(x)$,$c_{\mathrm{A}}(x)$ and $c_{\mathrm{B}}(x)$ in the model structure (see Figure 5) can be evaluated as

$$c_{\mathrm{A}}(x) = \frac{l_{\mathrm{ag}}(x)}{l_{\mathrm{fe}}(x)}\mu_0 \tag{21}$$

$$c_{\mathrm{B}}(x) = \frac{A(x)}{2\mu_0} \tag{22}$$

$$c_{\mathrm{H}}(x) = \frac{N}{l_{\mathrm{fe}}(x)}. \tag{23}$$

To identify the model parameters the magnet B of the hydraulic valve is separated and a load cell is mounted on a high precision positioning table (see Figure 6). The table allows to change the slider position and hence to change the air gap. Since the Jiles-Atherton model parameters can not be identified without a estimation approach, a loss function must be formulated. The measured values are converted by an analog to digital converter and hence a time-discret loss function is defined

$$L = \sum_{k=1}^{n} \left[F_{\mathrm{measured}}(k) - \hat{F}_{\mathrm{modelled}}(k)\right]^2. \tag{24}$$

The quadratic loss function L is minimized using a minimization algorithm [6]. Figure 7 shows the excitation signal that is used to identify the parameters. Because of the decreasing current amplitudes minor loops of the hysteretic characteristic are excited. The limiting curve as well as minor loops can be modelled employing the Jiles-Atherton model. In order to detect faults at the proportional valve with the underlying position control being active, the structure for closed-loop fault detection suggested in [7] is extended by two hysteresis models for the two DC magnets A and B. Because the stationary flow forces F_{V} can be very large, these forces should not be neglected. The flow forces (schematically shown in Figure 8) are also modelled and can be described by

$$F_{\mathrm{V}} = \rho Q_2 v_2 \cos(\varepsilon_2) - \rho Q_1 v_1 \cos(\varepsilon_1) \tag{25}$$

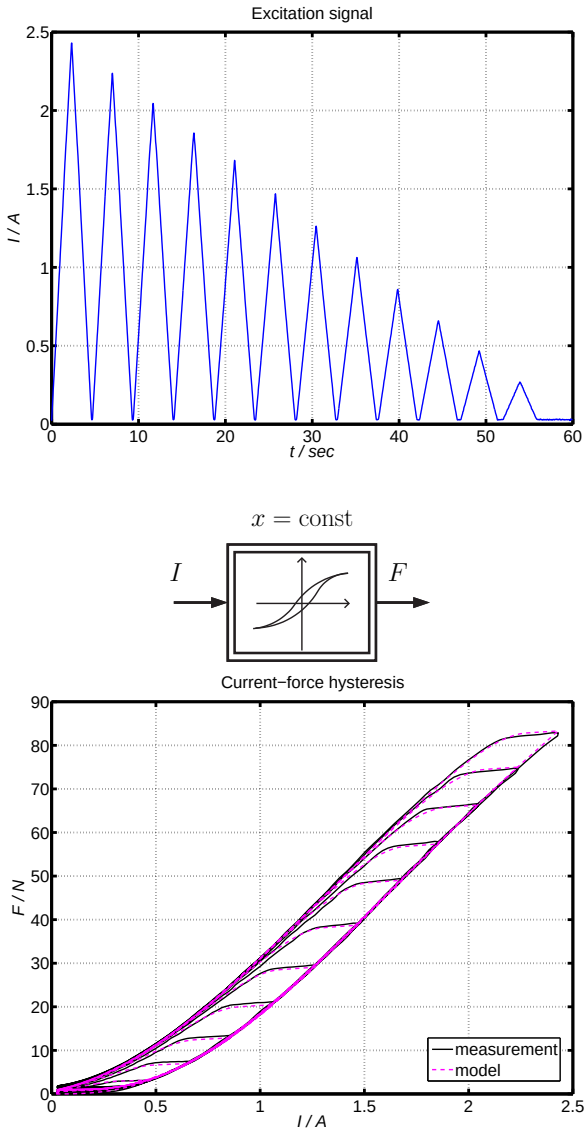

Figure 7. HYSTERESIS CURVE

with

ρ	:	fluid density
$Q_{1,2}$	:	volume flow (1,2)
$v_{1,2}$	:	velocity (1,2)
$\varepsilon_{1,2}$	:	jet angle (1,2)

The parameters of the flow force model are again identified with measurements on the testbed and parameter estimation methods. In order to generate the output residual r_1, Equation 9 must be considered. Additionally the dynamic performance of the position transducer system is modelled as a simple first-order time-delay element. The output residual is determined as the difference bewtween the measured slider position and the model output:

$$r_1 = y - \hat{y}. \tag{26}$$

Figure 9 shows the whole model structure that is used to detect

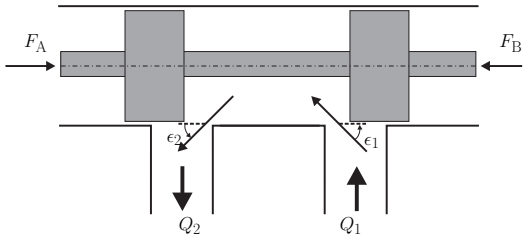

Figure 8. FLOW FORCES

faults in the hydraulic valve. The inputs are the two currents I_A, I_B and the modelled flow force F_V. The valve control structure on the testbed consists of two cascaded current controllers (coil A and coil B) and a superposed position controller. The coil currents must be measured because the cascaded current controller needs the information of the coil current. The currents are in general available and can be used for fault-detection. Hence no additional sensors are required to get the current signals. Figure 9 shows the model output $\hat{y}$, the measured slider position y as well as the residual r_1 for the fault-free case. The figure gives evidence that the two hysteresis models according to the Jiles and Atherton method allow to chose the thresholds for the residual very small even over a large operating range of the valve. Numerous experiments conducted on the testbed show that tiny, incipient faults can only be reliably detected using the hysteresis characteristics in the model. If the hysteretic effects are neglected the thresholds of the residual have to be chosen so large that small faults typically remain undetected, i.e. the residual remains below the thresholds. In the following the deflections of the residuals are shown using the example of a partial winding short and a current offset in coil A.

Fault 1: partial winding short (coil A)

As mentioned before the slider position is controlled by a position controller. The valve coils on the testbed are current controlled by two cascaded current controllers. If a partial winding short occurs in a coil, the cascaded current controller automatically adjusts the voltage at the H-bridge in order to reach the reference variable. After the fault occurs the superimposed position controller tries to reduce the control deviation by adjustment of the actuating variable ΔI. If the fault is small enough the actuating variable constraints are kept and the control loop covers the fault. The two coil currents are input signals of the new model structure (see Figure 9). Since the model parameters are identified for the fault-free case, the residual r_1 should deflect in case of a partial winding short. As expected the adjusted actuating variable ΔI generates a deflection in the residual r_1. Figure 10 shows the deflection of the residual r_1 in case of a partial winding short of 10% of the whole windings, which had been injected at $t = 5$sec in coil A. Due to the fact that the two currents supplied

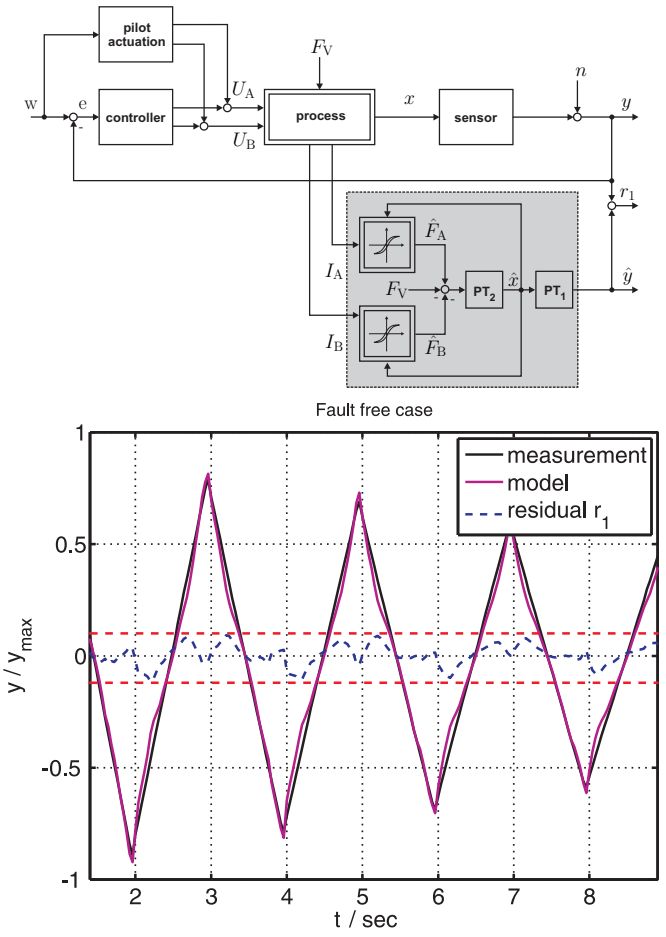

Figure 9. FAULT DETECTION IN CLOSED LOOPS

to the electromagnets are related by

$$I_A = I_0 - \Delta I \tag{27}$$

$$I_B = I_0 + \Delta I \tag{28}$$

with

I_0 : constant current (operation point)
ΔI : actuating variable

the fault can only be detected if the control input has not yet reached saturation, i.e. $\Delta I = I_0$ or $\Delta I = -I_0$. In the saturation, one of the two electromagnets does not carry any current, hence the partial winding short in the respective coil cannot be detected. This also explains, why the residual depicted in Figure 10 does not permanently remain outside the thresholds when a fault occurs. For a fault in electromagnet A, the residual crosses the upper threshold and for a fault in electromagnet B, it crosses the lower threshold. Not only the residual r_1 shows a deflection if a partial winding short occurs, but also the residual r_2 (see Equation 7) shows a deflection. In order to show the rise and fall of the currents the sample rate was chosen much higher. The partial winding short has been triggered injected at $t = 5$msec.

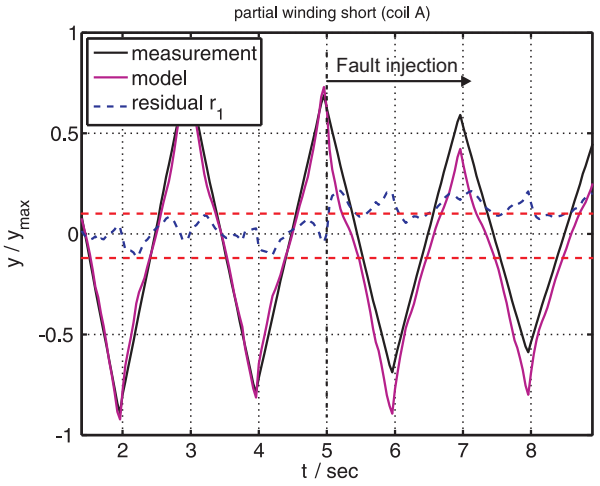

Figure 10. r_1 PARTIAL WINDING SHORT (COIL A)

Figure 11 shows, that in case of a partial winding short in coil A only the residual r_2 violates the thresholds, while r_3 (see Equation 8) remains within the thresholds. With signal-based methods (e.g. trend checking, limit checking etc.) the partial winding short can not be detected because the current controller compensates this fault. This is why the measured current signal I_A (see Figure 11) does not show any variation after the partial winding short. The fault-symptom table of this fault is shown in Table 1.

Fault 2: current sensor offset ΔI_A

As mentioned before the valve coils at the testbed are current controlled and the supply voltage of the H-bridges is much higher as needed to set the maximum coil current. The main reason for this control strategy is to increase the dynamic performance of the electromagnets. This over-excitation of the valve coil is uncritical in fault-free operation. But if there exists an offset between the real current and the measured current, the current controller sets up the wrong current. This can lead to overcurrent and in the worst case to an open fuse or even a burned coil. In order to detect the current offset

$$I_{A_{measured}} = I_A + \Delta I_A \quad (29)$$

$$\Delta I_A = 10\% \cdot I_{Amax} \quad (30)$$

in closed-loop operation the deflection of the three residuals are analysed. Since the coil currents are input signals of the magnetic models, the residual r_1 should deflect in case of a current sensor offset. The offset fault ($10\% \cdot I_{Amax}$) is triggered injected at $t = 5$sec. Figure 12 shows the deflection of residual r_1. The current sensor offset fault ($10\% \cdot I_{Amax}$) is injected at $t = 5$msec. As expected the current controller immediately adapts the voltage of the H-bridge (see dotted circle in Fig: 13) and adjusts the wrong measured current. Since the adapted voltage is an input

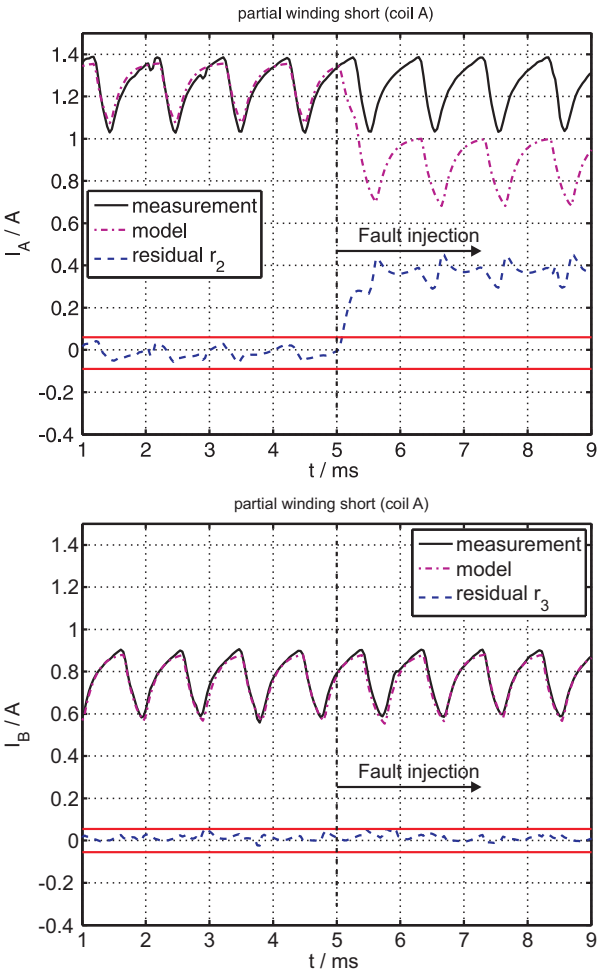

Figure 11. r_2,r_3 PARTIAL WINDING SHORT (COIL A)

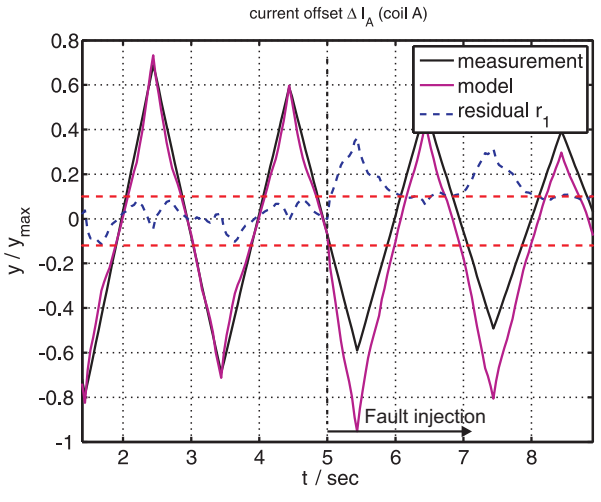

Figure 12. RESIDUAL r_1 CURRENT OFFSET ΔI_A (COIL A)

of the model, the residual r_2 should react. Figure 13 shows the

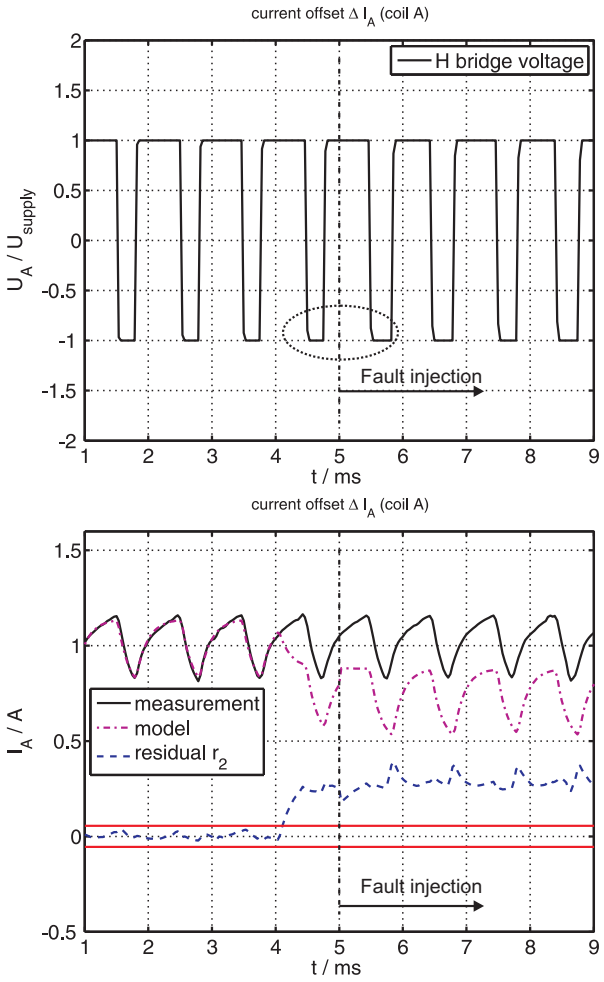

Figure 13. RESIDUAL r_2 CURRENT OFFSET ΔI_A (COIL A)

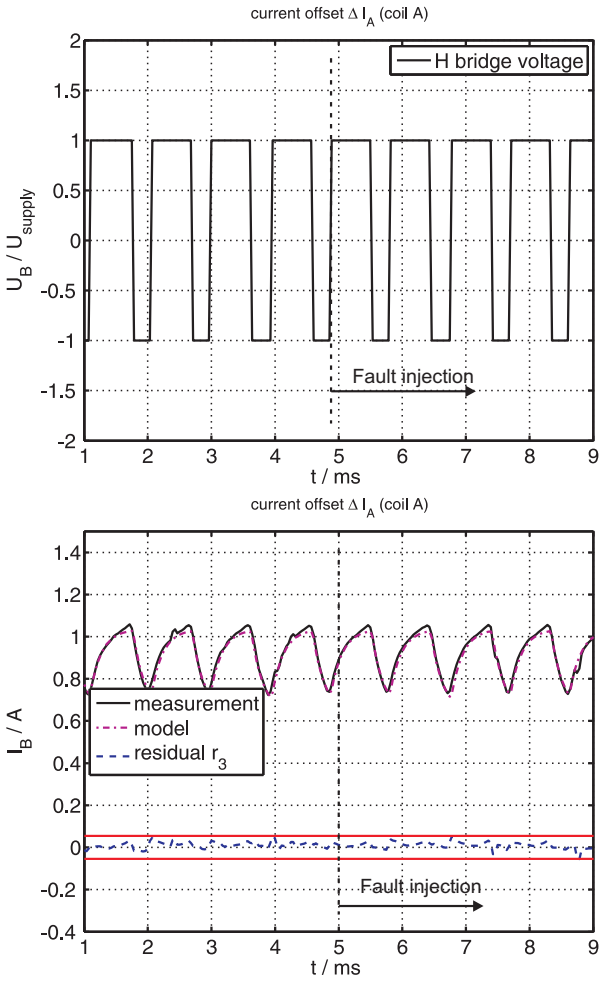

Figure 14. RESIDUAL r_3 CURRENT OFFSET ΔI_A (COIL A)

positive deflection of the residual r_2. As expected the residual r_3 does not deflect in case of a current offset fault ΔI_A. Figure 14 shows the square-wave voltage U_B, the appropiate current I_B as well as the residual r_3 in case of an offset current fault.

FAULT DIAGNOSIS

Table 1 shows that there exists a causality between the induced faults and the reaction of the residuals. The goal of the fault diagnosis is to derive the existence of faults from the observed symptoms. In general, there are two different approaches to the fault diagnosis. One is based on classification theory and the other on inference. The fault detection and diagnosis system described in this paper uses a fuzzy-logic based diagnosis approach. Fuzzy-logic allows to abandon the crisp separation of different states and uses a soft transition from one state to the other. The states are described by linguistic terms such as "reduced" or "increased". The heuristic knowledge about the causality between symptoms and faults is implemented to the diagnostic engine by means of IF-THEN rules. For a detailed description of fuzzy-logic systems consider e.g. [7]. Figure 15 shows the overall setup of the fuzzy-logic based diagnostic engine.

CONCLUSIONS

It has been shown that the precise modelling of the hysteresis of electromagnetic actuators by means of the Jiles-Atherton model allows to detect the presence of tiny, incipient faults in these actuators. The successful detection of a partial winding short of only 10% and also the detection of a current sensor fault has been shown in this paper with real experimental data recorded on the testbed. The methods developed in this paper are not only applicable to electromagnetic actuators, but also to other actuators with hysteretic behavior such as piezo actuators.

REFERENCES

[1] Inbook,Kallenbach, Eick, Quendt, Stroehla, Feindt,2005. *Elektromagnete. Grundlagen, Berechnung. Entwurf und Anwendung.*,2.Auflage. Vieweg Teubner, Wiesbaden

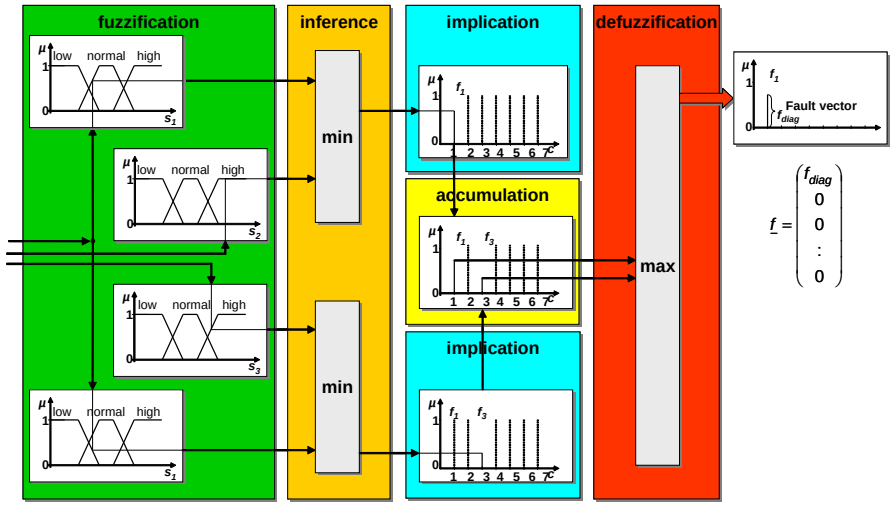

Figure 15. FUZZY DIAGNOSIS

Table 1. Fault-Symptom table

Fault	r_1	r_2	r_3
Partial winding short (coil A)	+	+	o
Partial winding short (coil B)	-	o	+
Current offset ΔI_A	+/-	+/-	o
Current offset ΔI_B	+/-	o	+/-
Overheated coil A	o	-	o
Overheated coil B	o	o	-
Blocked piston valve	+/-	o	o
Offset position sensor	+/-	o	o

o no deflection

\+ positive deflection

\- negative deflection

[2] Inbook,Suesse, R.,2005. *Theoretische Grundlagen der Elektrotechnik 1*, Vieweg Teubner, Wiesbaden

[3] Phdthesis,Muenchhof, M.,2006. *Model-Based Fault Detection for a Hydraulic Servo Axes* , Fortschritt Berichte VDI Reihe 8, Duesseldorf

[4] Inbook,Jiles, David.,1996. *Introduction to Magnetism and Magnetic Materials.* Chapman & Hall, London.

[5] Jiles, D.C., Atherton, D.L.,1986. "'Theory of ferromagnetic hysteresis."' *Journal of magnetism and magnetic materials Nr.61*,pp.48-60

[6] Inbook,Isermann, R.,1999. *Identifikation dynamischer Systeme. 1. Grundlegende Methoden.*, 2. Auflage, Springer Verlag, Berlin.

[7] Inbook,Isermann, R.,2006. *Fault-Diagnosis-Systems. An introduction from Fault Detection to Fault Tolerance.*, 2. Auflage, Springer Verlag, Berlin.

[8] Inbook,Isermann, R.,2008. *Mechatronische Systeme. Grundlagen*, 2. Auflage, Springer Verlag, Berlin.

[9] Phdthesis,Raab, U.,1993. *Modellgestuetzte digitale Regelung und Ueberwachung von Kraftfahrzeugen*, Fortschritt Berichte VDI Reihe 8, Duesseldorf